Representation of spontaneous movement by dopaminergic neurons is cell-type selective and disrupted in parkinsonism

Paul D. Dodson[a,b,1], Jakob K. Dreyer[c], Katie A. Jennings[d], Emilie C. J. Syed[a], Richard Wade-Martins[b,d], Stephanie J. Cragg[b,d], J. Paul Bolam[a,b], and Peter J. Magill[a,b,1]

[a]Medical Research Council Brain Network Dynamics Unit, Department of Pharmacology, University of Oxford, Oxford OX1 3QT, United Kingdom; [b]Oxford Parkinson's Disease Centre, University of Oxford, Oxford OX1 3QX, United Kingdom; [c]Department of Neuroscience and Pharmacology, University of Copenhagen, 2200 Copenhagen, Denmark; and [d]Department of Physiology, Anatomy and Genetics, University of Oxford, Oxford OX1 3QX, United Kingdom

Edited by Robert C. Malenka, Stanford University School of Medicine, Stanford, CA, and approved February 11, 2016 (received for review August 11, 2015)

Midbrain dopaminergic neurons are essential for appropriate voluntary movement, as epitomized by the cardinal motor impairments arising in Parkinson's disease. Understanding the basis of such motor control requires understanding how the firing of different types of dopaminergic neuron relates to movement and how this activity is deciphered in target structures such as the striatum. By recording and labeling individual neurons in behaving mice, we show that the representation of brief spontaneous movements in the firing of identified midbrain dopaminergic neurons is cell-type selective. Most dopaminergic neurons in the substantia nigra pars compacta (SNc), but not in ventral tegmental area or substantia nigra pars lateralis, consistently represented the onset of spontaneous movements with a pause in their firing. Computational modeling revealed that the movement-related firing of these dopaminergic neurons can manifest as rapid and robust fluctuations in striatal dopamine concentration and receptor activity. The exact nature of the movement-related signaling in the striatum depended on the type of dopaminergic neuron providing inputs, the striatal region innervated, and the type of dopamine receptor expressed by striatal neurons. Importantly, in aged mice harboring a genetic burden relevant for human Parkinson's disease, the precise movement-related firing of SNc dopaminergic neurons and the resultant striatal dopamine signaling were lost. These data show that distinct dopaminergic cell types differentially encode spontaneous movement and elucidate how dysregulation of their firing in early Parkinsonism can impair their effector circuits.

Parkinson's disease | dopamine | substantia nigra | ventral tegmental area | alpha-synuclein

Dopamine is vital for normal motor function, as exemplified by the motor deficits arising from the dysfunction/degeneration of midbrain dopaminergic neurons in Parkinson's disease (PD). One prevailing view is that midbrain dopaminergic neurons guide purposeful actions through encoding value, for example, by conveying the difference between expected and actual reward (1–3). Although this function has been ascribed to all midbrain dopaminergic neurons, there is considerable functional heterogeneity across different cell populations in the ventral tegmental area (VTA; A10) and the substantia nigra pars compacta (SNc; A9) (4–7). For example, some dopaminergic neurons respond to novel or salient events or during cognitive processes such as decision making and working memory (6, 8–10). Moreover, although the firing of these dopaminergic neurons generally has been thought not to vary consistently with movement (3, 11), there is evidence that the activity of putatively classified dopaminergic neurons can change during movement execution in a heterogeneous manner (12–16). This evidence, in turn, raises the possibilities that at least some types of movement might be differentially encoded by the firing of distinct populations of dopaminergic neuron and that dysregulation of such activity might contribute to motor impairment in PD before, or commensurate with, frank neurodegeneration.

To investigate whether and how different types of midbrain dopaminergic neurons represent movement, we recorded the firing of single dopaminergic neurons in awake, head-fixed mice during rest and spontaneous movement and then juxtacellularly labeled each recorded neuron to verify its cell type. We observed that identified SNc dopaminergic neurons typically paused their firing at the onset of movement, but VTA dopaminergic neurons did not. Using in silico simulations of dopamine-release dynamics, we show that brief, movement-related changes in dopaminergic neuron firing can be reliably "read out" in the striatum as robust changes in dopamine concentration and receptor signaling. Notably, movement-related pauses in SNc neuron firing and the resultant changes in dopamine signaling were lost in parkinsonian mice, further supporting a role for this patterned activity in movement.

Results

To define the activity of dopaminergic neurons with high spatiotemporal resolution during rest and movement, we extracellularly recorded action potentials fired by individual cells in untrained, head-fixed mice. Mice were placed on a running wheel, and recordings were made during rest or during brief (<1-s) spontaneous movements in which the mouse altered its position

Significance

Deciphering the roles of midbrain dopaminergic neurons in the control of movement is critical not only for understanding of normal motor function but also for defining the basis of motor dysfunction in Parkinson's disease. However the activity of these neurons generally has been considered to be unrelated to movement. Here we demonstrate that dopaminergic neurons signal the onset of spontaneous movement in a cell-type–selective manner and that these signals can be read out in transmitter and receptor activity dynamics in the striatum, one of their principal targets. Importantly, these movement-related signals were lost in a mouse model of Parkinson's disease. Together, these data suggest that movement-related firing of dopaminergic neurons is important for precise motor control.

Author contributions: P.D.D. and P.J.M. conceived and designed research with input from J.K.D., K.A.J., E.C.J.S., R.W.-M., S.J.C., and J.P.B.; P.D.D. performed all electrophysiological experiments and related analyses; J.K.D. performed computational modeling; K.A.J. performed voltammetry experiments; and P.D.D. wrote the paper with input from J.K.D., K.A.J., E.C.J.S., R.W.-M., S.J.C., J.P.B., and P.J.M.

The authors declare no conflict of interest.

This article is a PNAS Direct Submission.

[1]To whom correspondence may be addressed. Email: paul.dodson@pharm.ox.ac.uk or peter.magill@pharm.ox.ac.uk.

This article contains supporting information online at www.pnas.org/lookup/suppl/doi:10.1073/pnas.1515941113/-/DCSupplemental.

on the running wheel in the absence of any overt reward or other external cue (17). We focused our analyses on such movements for two reasons: (*i*) to avoid confounds arising from the challenges of distinguishing movement-related neuronal activity from that related to reward and/or external cues, and (*ii*) because brief movements were less likely to destabilize single-cell recordings and thus facilitated the subsequent juxtacellular labeling of neurons with Neurobiotin, which was used to locate recorded neurons unambiguously and to determine whether they were dopaminergic by post hoc assessment of tyrosine hydroxylase (TH) immunoreactivity (Fig. 1*A*). We reasoned that, despite the heterogeneous kinematics of such brief voluntary movements, any consistent neuronal responses that emerged would reflect general organizational or coding principles of dopaminergic neurons. In support of this notion,

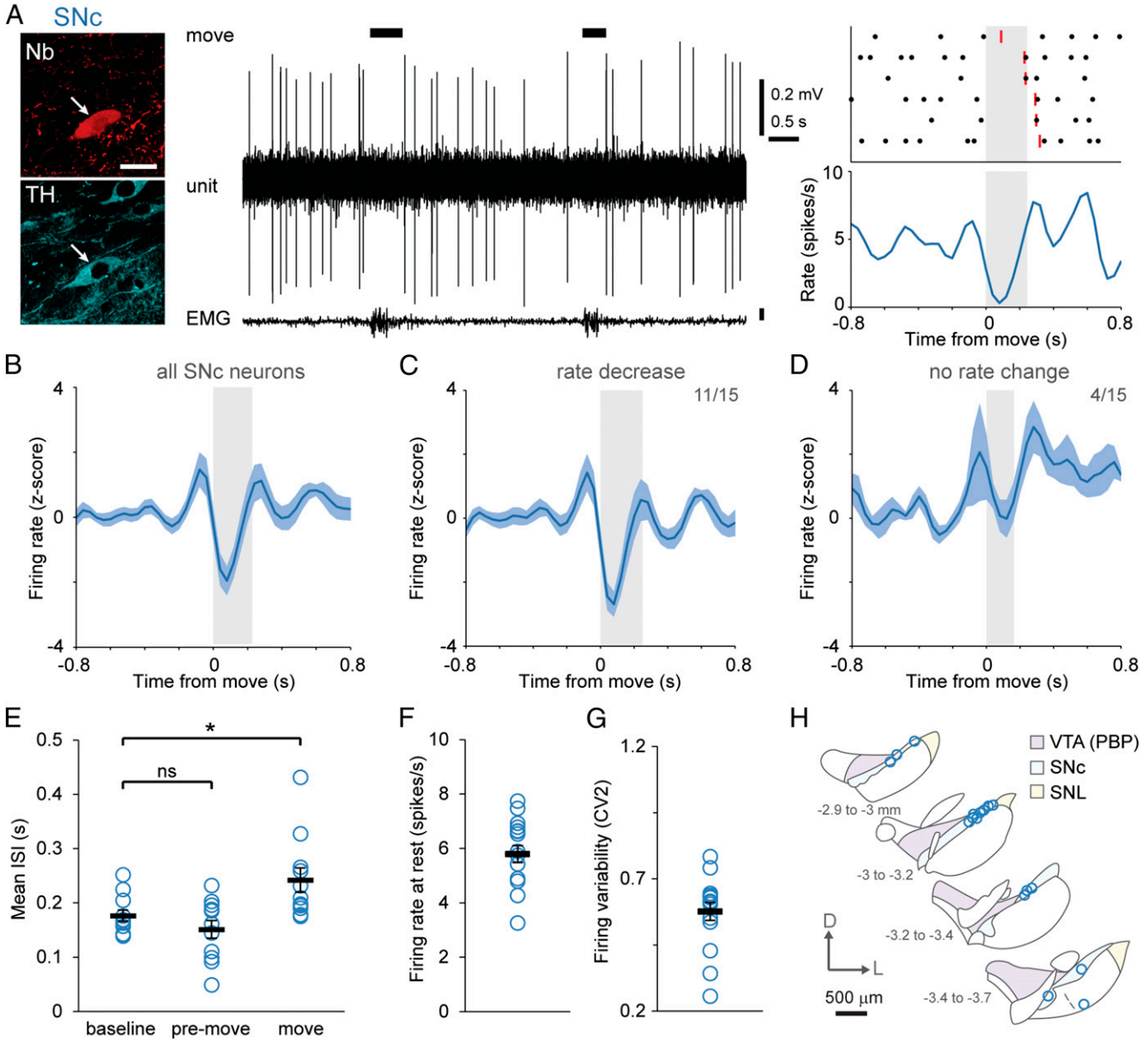

Fig. 1. Dopaminergic SNc neurons exhibit a pause in firing during the onset of spontaneous movement. (*A*) Example of single-unit activity (*Center*) and a peri-event time histogram (PETH) (*Lower Right*) with the corresponding raster plot from an identified dopaminergic SNc neuron (*Upper Right*) during rest and spontaneous movement, the latter denoted by black bars, determined from video and EMG activity. The ends of individual movement epochs are denoted in rasters by red lines, and the mean duration of movement is indicated by gray shading. (*Left*) After recording, each neuron was juxtacellularly labeled with Neurobiotin (Nb) to identify its dopaminergic nature (by immunoreactivity to TH) and to confirm its location. (Scale bar, 20 µm.) (*B–D*) Mean normalized PETHs ± SEM. On average, SNc neurons ($n = 15$) transiently increased their activity just before movement and then paused their firing at the movement onset (*B*); 11 SNc neurons significantly decreased their rate during movement onset (*C*), and four did not change their rate significantly (*D*). (*E*) Mean interspike intervals (ISIs) during the baseline, premovement (ISIs ending in the 100 ms before movement), and movement (ISIs starting in the 100 ms preceding movement and ending after movement onset) periods. The ISI during movement onset was significantly longer than baseline ISIs [$P < 0.01$, $n = 11$ neurons that met analysis criteria (*SI Materials and Methods*), one-way repeated-measures ANOVA with Dunnett's post hoc comparison]. (*F* and *G*) Firing rate (*F*) and variability quantified by CV2 (*G*) of all SNc neurons ($n = 16$) during alert rest. (*H*) Schematic coronal sections denoting locations within the SNc of all recorded and identified dopaminergic neurons. Adapted from ref. 50. The distance from bregma is shown on left. D, dorsal; L, lateral; PBP, parabrachial pigmented area of the VTA. Data are presented as mean ± SEM; *$P < 0.05$; ns, not significant.

we observed that the majority of identified SNc dopaminergic neurons dramatically and consistently reduced their firing rate at movement onset (Fig. 1 *A* and *B*).

The Firing Rate of Most SNc Dopaminergic Neurons Decreases at Movement Onset. To compare movement-related changes in firing rate between neurons, we converted firing rates to z-scores; when all SNc neurons ($n = 15$) were considered together, they exhibited a significant decrease in their mean population firing rate at movement onset (Fig. 1*B*). When considered individually, 11 of 15 SNc dopaminergic neurons showed significant decreases in firing rate during movement onset (defined as the first 160 ms of each movement) (Fig. 1*C*); the remaining four neurons showed no change during the onset period (Fig. 1*D*). A minority of all SNc neurons (4/15) exhibited significant rate increases during the premovement period (160 ms immediately preceding movement); however, these neurons also exhibited decreases in mean firing at movement onset (Fig. S1*A*). Importantly, the occurrence of a movement-related pause in firing was not dependent on any premovement rate increase (Fig. S1*B*), suggesting that the pause was not simply a refractory period following any increased firing just before movement. Comparison of interspike intervals (ISIs) confirmed a genuine pause in firing (Fig. 1*E*): The mean ISI during movement onset was significantly longer than that during baseline, but baseline and premovement ISIs were similar. To examine further whether the firing-rate variations of SNc neurons around brief movements were sufficiently distinct from stochastic rate changes occurring between movements, we analyzed the area under the receiver operating characteristic (AUROC) curve of each SNc neuron to test whether the firing rate of each neuron could be used to correctly classify the occurrence of spontaneous movements. The firing of most SNc neurons (11/15) predicted movement significantly above chance (mean AUROC of 0.65 ± 0.02; $n = 11$), suggesting that their firing-rate variations around movement are distinct enough to encode information.

We also explored whether SNc dopaminergic neurons represented the end of a movement, but we found no significant changes in firing rate following movement (Fig. S2*A*), suggesting that the activity we observe specifically signals the onset of movement rather than indiscriminately representing a transition between states of mobility and immobility. To examine whether decreases in SNc neuron firing rates at movement onset were specific to brief movements, we also analyzed neuronal activity recorded during longer spontaneous movements (>1 s), which typically involved the animal walking or running on the wheel. The decreased firing of SNc neurons that occurred at the onset of brief movements also occurred at the onset of the long-duration movements (Fig. S2*B*), confirming that movement representation by SNc neurons extends to different types of spontaneous movement. We recorded neurons at different locations within the SNc (Fig. 1*H*) but found no significant relationships between the firing properties and the mediolateral (ML) or anteroposterior (AP) SNc locations of the neurons we sampled (Fig. S3). Taken together, these data show that most SNc dopaminergic neurons encode spontaneous movement with a pause in firing.

Distinct Dopaminergic Cell Types Differentially Encode Movement. Experiments in primates have shown that the responses of putatively classified dopaminergic neurons to task-related stimuli vary according to the neurons' location along an ML axis (4, 8). We hypothesized that the encoding of spontaneous movement by dopaminergic neurons might be cell-type selective. The precise localization of recorded neurons (afforded by juxtacellular labeling) allowed us to test this hypothesis unambiguously. Thus, in addition to SNc neurons, we also recorded responses from dopaminergic neurons in the lateral VTA (the parabrachial pigmented area) (Fig. 2 *A*, *B*, and *G*) and the substantia nigra pars lateralis (SNL) (Fig. 2 *C*, *D*, and *G*). Dopaminergic SNc neurons predominantly innervate the dorsal striatum, whereas lateral VTA neurons preferentially project to the nucleus accumbens, and SNL neurons project to several limbic targets (18). During periods of alert rest, VTA and SNL neurons fired at rates similar to those of SNc neurons (Figs. 1*F* and 2*E*; $P > 0.05$, $n = 14$ VTA neurons, 5 SNL neurons, and 16 SNc neurons, one-way ANOVA), but the firing of SNL neurons was significantly more irregular [as assessed by the coefficient of variation of the ISI (CV2)] than that of SNc neurons ($P < 0.05$, ANOVA on ranks with Dunn's post hoc test) (Figs. 1*G* and 2*F*). Unlike SNc neurons, neither VTA nor SNL neurons showed significant average responses during the movement-onset period (Fig. 2 *B* and *D*). A minority of VTA dopaminergic neurons (5/14) and most SNL neurons (4/5) increased their firing rate significantly immediately preceding movement (Fig. S1), resulting in average premovement increases at the population level (Fig. 2 *B* and *D*). These differences in the timing, polarities, and relative magnitudes of responses of SNc, VTA, and SNL neurons did not arise from any systematic differences in the movements recorded with each cell type (average duration of movement: $P > 0.05$, ANOVA on ranks). Taken together, these data indicate that the firing of midbrain dopaminergic neurons around spontaneous movements is cell-type selective.

Brief Pauses in SNc Neuron Firing Cause Transient Reductions in Striatal Dopamine Levels. It is important to understand whether behavior-related changes in the firing of populations of dopaminergic neurons translate to fluctuations in striatal dopamine concentration. Currently, in vivo detection of increases and decreases of extracellular dopamine concentration at subsecond resolution [i.e., with fast-scan cyclic voltammetry (FCV)] has not been well established in the dorsal striatum. To overcome this limitation, we used a biophysical computational model of dopamine release recently developed for rat striatum (19–21). We adjusted SNc neuron innervation to model the dorsolateral mouse striatum (22) but left all other parameters unchanged. Using the spike trains of all our recorded SNc neurons as inputs for the model, we examined how SNc neuron firing shaped dopamine release relative to movement (Fig. 3*A*). The model predicted that the baseline firing of SNc neurons results in a dopamine tone of ∼60 nM (Fig. 3*B*). Transient increases in the average firing of SNc neurons immediately preceding movement (see above) caused a significant increase in dopamine concentration (∼20 nM). This increase was followed by a significant decrease in dopamine (∼20 nM below baseline) during movement onset (Fig. 3*B*), i.e., the point at which SNc neurons paused. To test whether such decreases were biologically plausible, we used FCV to measure the extracellular dopamine concentration in the dorsal striatum ex vivo (evoked by local stimulation at 6 Hz to approximate the baseline firing rate of SNc dopaminergic neurons; see Fig. 1*F*). Brief pauses in stimulation [similar in duration to the ISI during movement onset (Fig. 1*E*)] resulted in significant decreases in the extracellular dopamine concentration (∼20 nM) (Fig. S4), indicating that movement-related pauses in neuron firing can indeed be reported as changes in striatal dopamine.

Our model predicts that movement-related firing of SNc neurons will alter dorsal striatal dopamine levels immediately before and during movement onset. However, the effect that this alteration has on striatal neurons will depend on the dopamine receptors that they express. Striatal spiny projection neurons (SPNs) can be grossly subdivided into direct pathway SPNs (dSPNs), which express D1 dopamine receptors, and indirect pathway SPNs (iSPNs) that express D2 receptors (23). Although both D1 and D2 receptors can exist in high-affinity and low-affinity states (24), intracellular signaling cascades in dSPNs appear to be activated by high levels of dopamine via D1 receptors, whereas intracellular signaling in iSPNs is inhibited by basal levels of dopamine acting

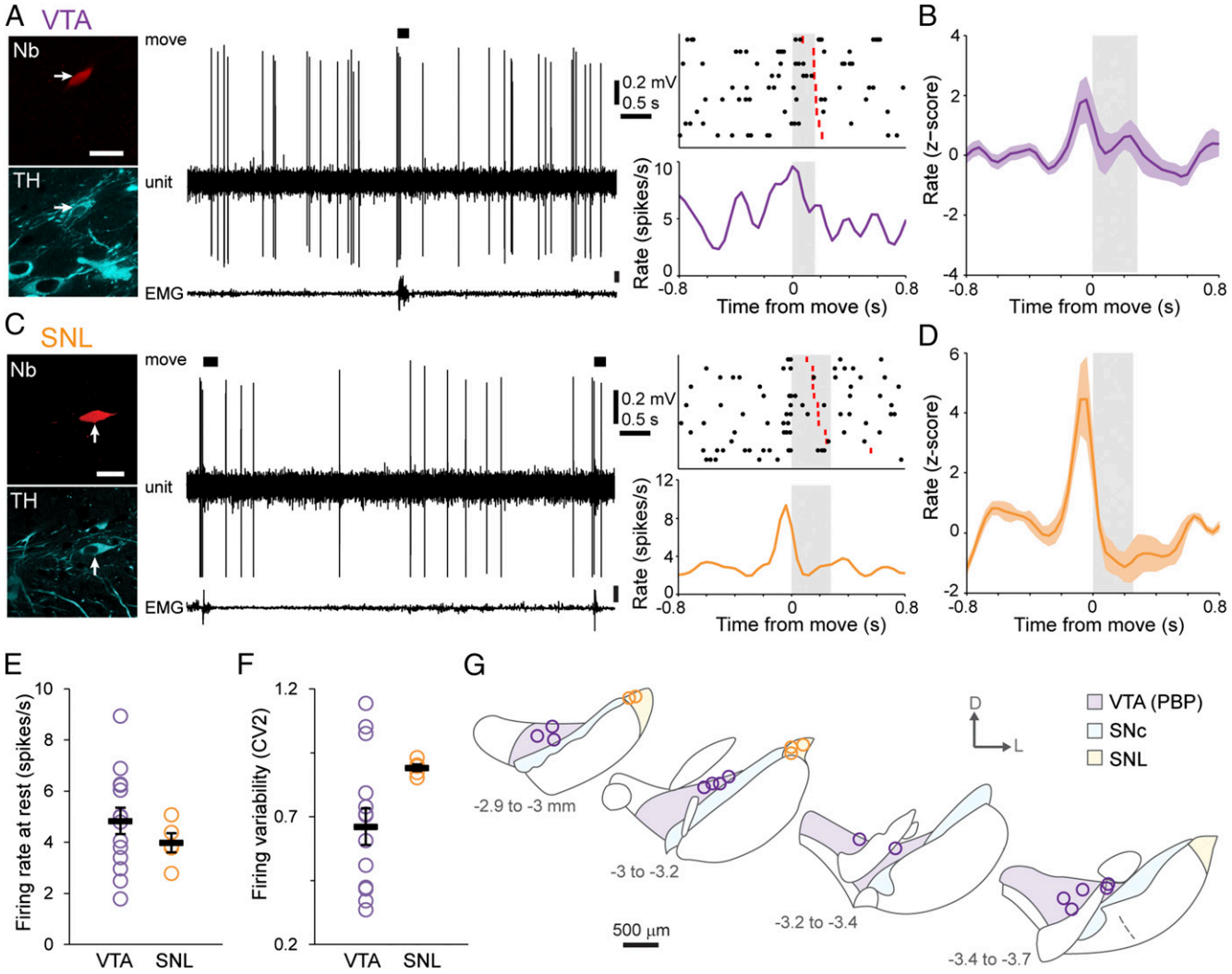

Fig. 2. The firing rate of VTA and SNL dopaminergic neurons does not change during movement onset. (*A* and *C*) Examples of single-unit activities and PETHs from identified dopaminergic neurons in the VTA (*A*) and SNL (*C*). (Scale bars, 20 μm.) (*B* and *D*) Mean normalized PETHs of all dopaminergic neurons in the VTA (*B*) and SNL (*D*). On average, neurons transiently increased their firing rates just before movement but did not significantly change firing during the movement period itself (gray shading). (*E* and *F*) Mean firing rate (*E*) and regularity of firing rate (*F*) of VTA and SNL dopaminergic neurons during alert rest (n = 14 VTA neurons and 5 SNL neurons). (*G*) Schematic coronal sections denoting the locations of all recorded and identified neurons in the VTA (purple) or SNL (orange). Data are presented as mean ± SEM.

at D2 receptors (25, 26). We therefore used the model to examine how the predicted movement-related changes in striatal dopamine concentration would activate low-affinity (EC_{50} = 1 μM) D1 receptors and high-affinity (EC_{50} = 10 nM) D2 receptors. The predicted activity of D1 receptors closely matched the dopamine concentration profile, resulting in a small but significant increase in D1 receptor activity preceding movement followed by a significant decrease during movement onset (Fig. 3*C*). Because D2 receptor activity was high at rest, the increase in dopamine concentration preceding movement was not matched by a significant increase in D2 receptor activity (Fig. 3*D*). However, the predicted decrease in dopamine concentration during movement onset resulted in a proportionally larger decrease in D2 receptor activity (~15%) (Fig. 3*D*). It recently has been demonstrated that D2 receptors coupled to exogenous G protein-coupled inwardly rectifying potassium channels can exist in a low-affinity state (27). Our model indicates that any low-affinity D2 receptors would be sensitive not only to the pause in SNc neuron firing but also to the premovement increase in dopamine.

The movement-related responses of VTA neurons differed from those of SNc neurons. Therefore we modeled how VTA neuron firing would affect dopamine signaling in their principal target, the nucleus accumbens. In contrast to the scenario simulated for the dorsal striatum receiving SNc neuron inputs, dopamine concentration and D1 receptor activity in the nucleus accumbens peaked during movement, but D2 receptor activity was unchanged during movement (Fig. S5). Taken together, these data illustrate how brief, movement-related changes in the firing rates of midbrain dopaminergic neurons can lead to rapid and robust changes in striatal dopamine signaling. However, our data reiterate that the precise nature of movement-related signaling depends on the type of neuron providing inputs (SNc vs. VTA), the striatal region innervated (dorsal striatum vs. accumbens), and the type of dopamine receptor expressed by striatal neurons (D1 vs. D2).

Movement-Related Pauses in SNc Neuron Firing Are Lost in Parkinsonian Mice. Our experiments described above indicate that the movement-related pauses in SNc neuron firing and the associated changes in

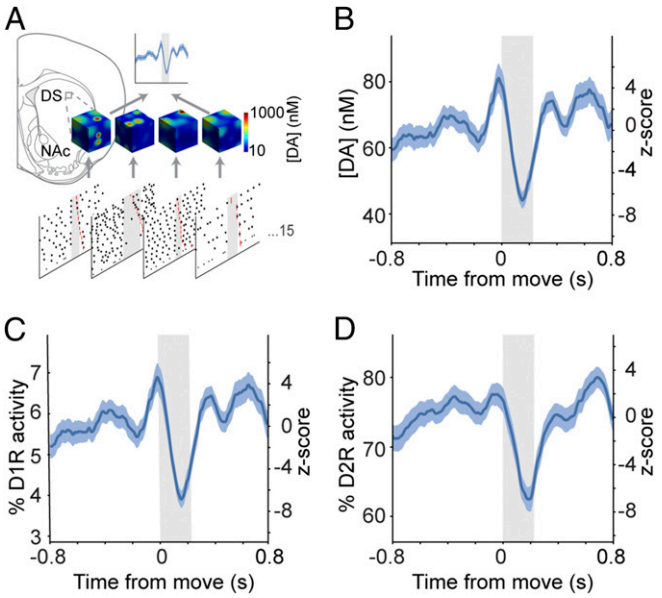

Fig. 3. Movement-related firing of SNc neurons significantly alters dopamine signaling in the dorsal striatum. (*A*) Schematic of the computational model of dorsal striatal dopamine signaling. Dopamine release and receptor activity in an ∼25-μm^3 area of the dorsal striatum (DS) was modeled using movement-related activity from each recorded SNc neuron (n = 15) as exemplified by snapshot concentration plots. Single-neuron responses were then averaged to generate population-level estimates of dopamine concentration. NAc, nucleus accumbens. (*B*) Mean peri-movement dopamine concentrations. Note the decrease in dopamine timed with movement onset. (*C* and *D*) Peri-movement activity profiles of low-affinity D1 dopamine receptors (*C*) and high-affinity D2 dopamine receptors (*D*). Mean response ± SEM is plotted on the left axes; the z-score is plotted on the right axes.

striatal dopamine release could be important for signaling movement. Thus, one might expect that such firing patterns would be altered when movement and dopamine neuron function are abnormal, e.g., in PD. To test this prediction, we used a transgenic mouse model of PD (*SNCA*-OVX mice) in which moderate overexpression of human α-synuclein (a human-disease–relevant genetic burden) leads to a slow, progressive phenotype that recapitulates many of the cardinal features of PD (28). Although aged *SNCA*-OVX mice have normal gross motor function (i.e., they perform spontaneous movements), they have impaired motor precision, resulting in foot-slips on the balance beam (28). To assess the neural representation of movement in these parkinsonian mice, we recorded and labeled SNc dopaminergic neurons in aged (23- to 27-month-old) *SNCA*-OVX mice and their littermate controls (*Snca*$^{-/-}$ mice). We have reported previously that the mean firing rate of SNc neurons is ∼30% lower in anesthetized *SNCA*-OVX mice than in littermate controls (28), and we found that this phenotype was maintained in awake mice during alert rest (Fig. S6). At movement onset, SNc neurons in *Snca*$^{-/-}$ littermate controls exhibited the same average reduction in firing rate seen in wild-type mice (P > 0.05, n = 15 neurons in wild-type mice and 11 neurons in *Snca*$^{-/-}$ mice, Mann–Whitney rank sum test), with 8 of 11 neurons showing significant decreases in firing rate (Fig. 4 *A* and *B*). Correspondingly, the mean ISI of these neurons during movement onset also was longer than the ISIs during baseline and premovement periods (Fig. 4*E*). In contrast to control mice, the mean movement-related firing of SNc neurons in the parkinsonian *SNCA*-OVX mice was not significantly different from baseline (Fig. 4*D*). Furthermore, ISIs at movement onset were not significantly longer than at baseline (Fig. 4*F*). Only 4 of 12 SNc neurons in *SNCA*-OVX mice exhibited significant decreases in rate, with the remaining neurons showing either no movement-related changes (5/12) or aberrant rate increases at movement onset (3/12; such increases were not observed in wild-type or *Snca*$^{-/-}$ mice). To ensure that this loss of movement-related reduction in the firing of *SNCA*-OVX dopaminergic neurons was not the result of a floor effect from their lower firing rates, we calculated the threshold rate that each neuron would need to cross to reach significance. For 11 of 12 neurons, the threshold was above the lowest mean firing rate observed in *SNCA*-OVX mice during onset, suggesting that they had not hit a floor in their firing rate (the remaining neuron increased its firing rate significantly at onset). In summary, these data provide the first direct evidence, to our knowledge, that the real-time encoding of behavior by the firing of surviving dopaminergic neurons is perturbed in parkinsonism.

Defining how altered movement-related firing of dopaminergic neurons affects striatal dopamine dynamics is essential for understanding the neuronal basis of the motor symptoms of PD. We therefore input spike trains recorded from all SNc neurons in littermate control and parkinsonian mice into our computational model. Dopamine signaling modeled in the dorsal striatum of control *Snca*$^{-/-}$ control mice was similar to that in wild-type mice, with striatal dopamine concentration, D1 receptor activity, and D2 receptor activity decreasing at movement onset (Fig. 5 *A*–*C*). However, when dopamine signaling was modeled using spike trains recorded from *SNCA*-OVX mice, not only was the dopamine tone lower at rest (as would be expected, given the lower firing rate of SNc neurons in these mice), but also there were no significant movement-related decreases in dopamine concentration or receptor activity (Fig. 5 *A*–*C*). These findings suggest that in the parkinsonian mice the loss of movement-related dopaminergic neuron firing is reflected in the striatum as abnormally static dopamine release during movement. Aged *SNCA*-OVX mice not only exhibit altered SNc neuron firing but also lose ∼30% of their dopaminergic SNc neurons, and their ability to release dopamine in the dorsal striatum is impaired (28). To examine how these two additional deficits might interact with aberrant movement-related SNc neuron firing in parkinsonian mice, we incorporated these abnormalities into the model. The cumulative effect was even lower dopamine tone and receptor activity and further blunting of the modeled movement-related dopamine signaling in the striatum (Fig. 5 *D*–*F*).

Discussion

Here, we define changes in the firing of neurochemically identified dopaminergic neurons around the onset of spontaneous movement. We show a pause in firing at movement onset in SNc neurons and an increase in the mean activity of VTA and SNL neurons just before movement. Importantly, our in silico modeling predicts that these movement-related changes in SNc neuron firing will be read out in the dorsal striatum as rapid and robust changes in dopamine concentration and receptor signaling. Moreover, the movement-related pause in SNc neuron firing and resultant changes in dopamine signaling are lost in parkinsonian mice, suggesting that these fine temporal dynamics are important for motor control.

Although the role of dopaminergic neurons in encoding reward, salience, and aversion is well established, the prevailing view from task-based recordings in primates is that dopaminergic neuron firing does not systematically change on fine time scales during movement (3). However, recent reports suggest that the firing of putative dopaminergic neurons in both rodents and primates is altered during trained movements (12–15). Our data show that the activity of identified dopaminergic neurons (in the SNc, VTA, and SNL) also changes around the spontaneous movements made by untrained mice in the absence of any overt cues or reward. Recordings of putative dopaminergic neurons have reported diversity in the polarity of movement-related rate changes, with some neurons increasing and others decreasing their firing rate (14, 15). Framing such diversity in terms of identified cell types is clearly important. By unambiguously defining the locations and neurochemical properties of our recorded neurons

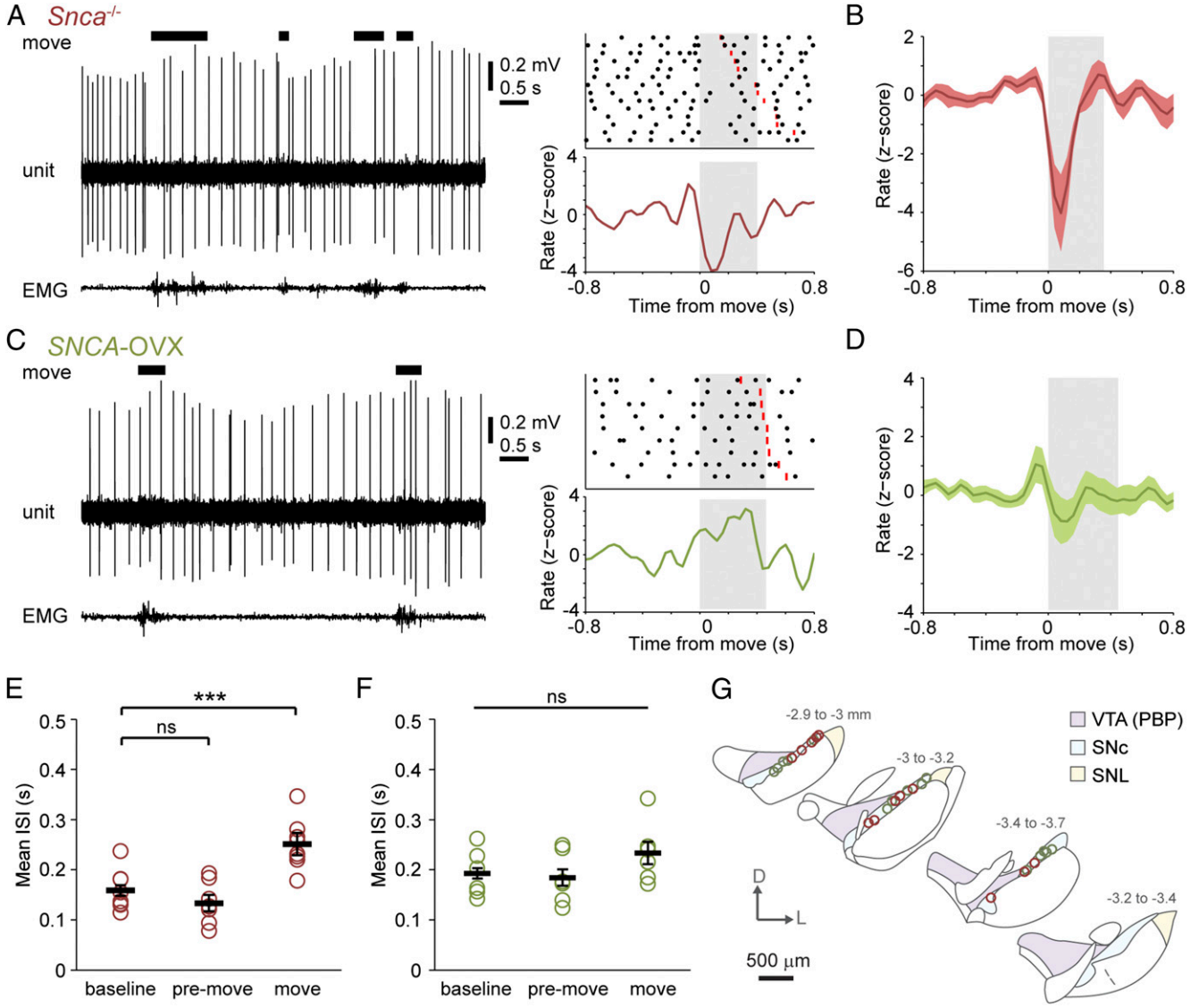

Fig. 4. Dopaminergic SNc neurons in parkinsonian mice do not reliably represent movement onset in their firing rates. (*A* and *C*) Examples of single-unit activities and PETHs from identified dopaminergic SNc neurons in 2-year-old *Snca*$^{-/-}$ littermate controls (*A*) and *SNCA*-OVX parkinsonian mice (*C*). (*B* and *D*) Mean PETHs show that, on average, the firing rate of SNc neurons in *Snca*$^{-/-}$ mice ($n = 11$ neurons) decreased significantly at movement onset (*B*), but there was no significant change in the firing rate of SNc neurons in *SNCA*-OVX mice ($n = 12$ neurons) (*D*). (*E*) Mean ISIs of neurons in *Snca*$^{-/-}$ mice during the baseline, premovement, and movement periods (defined as in Fig. 1); ISIs were significantly longer during movement than at baseline ($P < 0.001$, $n = 8$ neurons, one-way repeated-measures ANOVA with Dunnett's post hoc comparison). (*F*) ISIs were not significantly different in *SNCA*-OVX parkinsonian mice ($P > 0.05$, $n = 6$ neurons, one-way repeated-measures ANOVA). (*G*) Schematic coronal sections denoting locations of recorded and labeled neurons within the SNc [$n = 13$ neurons from *Snca*$^{-/-}$ mice (red) and 14 neurons from *SNCA*-OVX mice (green)]. Data are presented as mean ± SEM; ***$P < 0.001$; ns, not significant.

(using juxtacellular labeling), we demonstrate that distinct dopaminergic cell types respond differently during discrete phases of movement: SNc neurons represent the onset of movement with a pause in their firing, whereas VTA and SNL neurons show no change in firing rate during this period. Dopaminergic neurons exhibit heterogeneity not only in their properties and connectivity (5–7, 29–32) but also functionally, with medially located neurons signaling value and more lateral neurons encoding salience and cognitive significance (4, 8, 33). Here, we advance the notion of functional heterogeneity by showing that some modalities encoded by dopaminergic neurons can be defined according to well-circumscribed subpopulations rather than as a spatial gradient in signaling.

Previous work has shown that some dopaminergic neurons signal aversion (or cues predicting it) through a reduction in firing rate (5, 34, 35). Several lines of evidence suggest that the movement-associated decreases in the firing of SNc neurons that we observed are not related to aversion or a negative prediction error. First, compared with VTA neurons (4, 6, 34–36), SNc neurons exhibit relatively poor encoding of aversive stimuli and negative prediction errors (37–39). Moreover, we observed movement-related decreases in the firing of SNc neurons but not of VTA neurons, the opposite of what would be expected if the pauses were encoding aversion. Second, not only did fewer SNc neurons in parkinsonian mice display movement-related decreases in firing; some neurons actually increased firing. If pauses in firing were encoding aversion or prediction errors, one would expect to observe the same pauses in *SNCA*-OVX mice, because these mice do not have abnormal anxiety or cognitive phenotypes (28). Thus, our findings support work showing that some dopaminergic

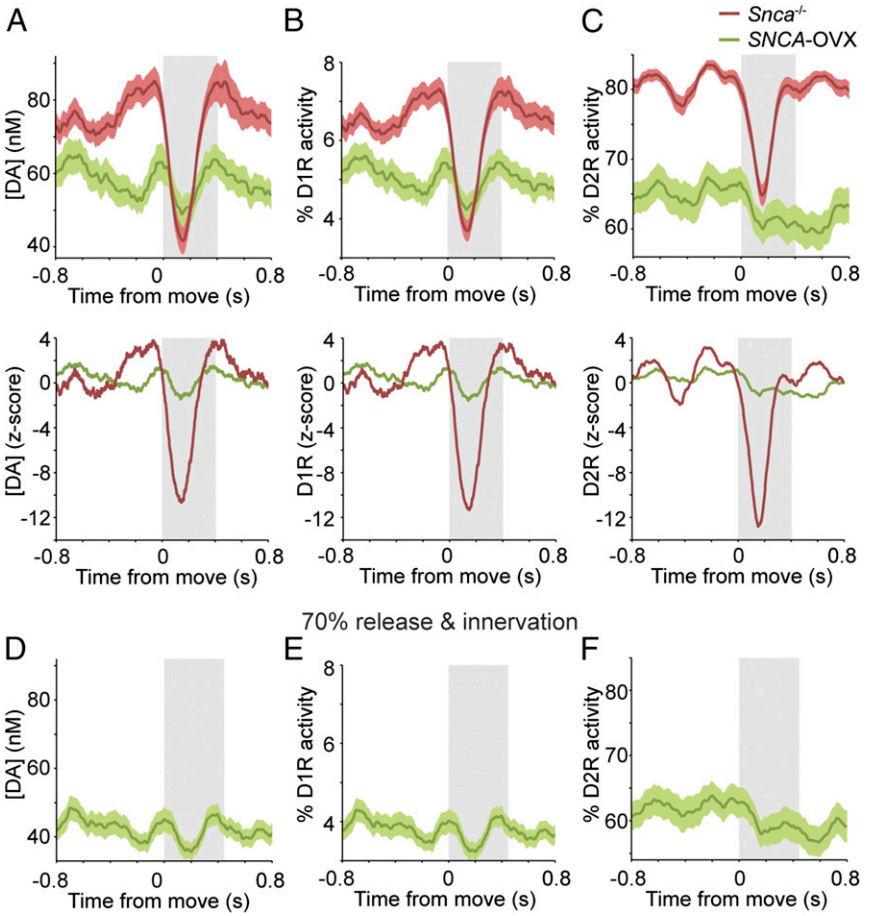

Fig. 5. Movement-related changes in striatal dopamine signaling are lost in parkinsonian mice. (*A*, *Upper*) Dorsal striatal dopamine concentrations (mean responses ± SEM) simulated using movement-related activity from SNc neurons recorded in Snca$^{-/-}$ littermate controls (red) or in parkinsonian *SNCA*-OVX mice (green). (*Lower*) Corresponding z-scores. (*B* and *C*, *Upper*) Activity of low-affinity D1 receptors (*B*) and high-affinity D2 dopamine receptors (*C*). (*Lower*) Corresponding z-scores. (*D*–*F*) Dopamine concentration (*D*), D1 receptor activity (*E*), and D2 receptor activity (*F*) modeled with parameters adjusted to match deficits present in aged *SNCA*-OVX mice (the abnormally low firing rate of SNc neurons plus a 30% reduction in dopamine release and dopaminergic innervation).

neurons can use decreases in firing rate for encoding information (4, 6, 34–36) and extend this concept to include their representation of spontaneous movement. It would be important to test in the future whether our findings extend to trained animals performing movement sequences embedded in a temporal framework of cues and rewards (e.g., in operant tasks).

Because dopaminergic neurons fire in the absence of excitatory synaptic inputs (7), the movement-related reduction in firing rate of SNc neurons is likely to be mediated by increased inhibitory input rather than by suppression of excitatory drive (40). Around 50% of synapses made with SNc neurons are GABAergic (41), and these originate from numerous sources including the substantia nigra pars reticulata (SNr), the globus pallidus, the superior colliculus, the rostromedial tegmental nucleus, and SPNs located in striosomes (33, 42). However, it has yet to be determined which of these diverse afferents convey appropriately timed, movement-related signals to inhibit dopaminergic neuron firing.

Because reduced dopamine levels in PD are ostensibly antikinetic, one might have expected a priori that dopaminergic neurons would increase their firing during movement; instead, we find movement-related decreases in SNc neuron firing. What then is the role of these movement-related pauses in firing? *SNCA*-OVX mice show a loss of movement-related SNc neuron firing in association with a loss of motor precision; however, these mice, which model early stages of parkinsonism, do not show gross motor abnormalities. As such, pauses in firing may not be necessary for the initiation of movement but instead might be important for the precision of movement. Although dopamine is generally thought to play an indirect modulatory role in shaping the accuracy of future movements (43), it is worth noting that the timescale at which dopamine acts at downstream molecular effectors [with activation of striatal D2 autoreceptors or potassium channels occurring at around 50 ms (27, 44)] is consistent with dopamine's having a role in supporting the selection of ongoing movements. Our computational model indicates that dorsal striatal D2 receptor activity would be disproportionately impacted by pauses in SNc neuron firing, thereby reducing D2 receptor-mediated suppression of iSPN activity in the dorsal striatum. In models of action selection (45, 46), such disinhibition is thought to suppress competing movements, and thus pauses in firing could act to maintain movement precision. This said, our data also suggest this scheme might not hold in the ventral striatum; the representation of movement by VTA and SNc dopaminergic neurons is different, and the resultant dopamine signaling in the nucleus accumbens should be distinct from that in the dorsal striatum. Moreover, accumbens SPNs are not as clearly organized into direct and indirect pathways (47). Further complexity arises from the recent finding that dopaminergic VTA and SNc neurons also corelease GABA (48). Although the influence of GABA release caused by baseline firing of dopaminergic neurons in vivo is not yet clear, one might expect GABA release resulting from premovement SNc neuron firing to contribute to the inhibition of both dSPNs and

iSPNs, which then would be disinhibited at movement onset by the pause in SNc neuron firing. Such patterns of inhibition might be expected to sharpen and coordinate dSPN and iSPN activity.

In conclusion, we show that midbrain dopaminergic neurons can encode spontaneous movement with temporally precise changes in their firing and that such encoding is cell-type selective. Neurons located in the SNc, the dopaminergic cell population that is particularly vulnerable to degeneration in PD (49), signal movement onset with a pause in firing, whereas more resistant populations (in the VTA and SNL) do not. Alteration of the movement-related firing of SNc neurons and the resultant loss of dopamine signaling in experimental parkinsonism suggest that the activity dynamics we define here are important for the control of voluntary movement.

Materials and Methods

All experimental procedures on animals were conducted in accordance with the Animals (Scientific Procedures) Act, 1986 (United Kingdom), and approved by local ethical review at the Department of Pharmacology, University of Oxford. Experiments were performed using 3- to 4-month-old male C57Bl6/J mice or 23- to 27-month-old male *SNCA*-OVX mice and male *Snca*$^{-/-}$ littermates.

In Vivo Electrophysiological Recording, Juxtacellular Labeling, and Data Analysis. Extracellular recordings were made from individual dopaminergic neurons in head-fixed mice positioned on an Ethofoam running wheel (17). After recording, each neuron was juxtacellularly labeled with Neurobiotin (17, 28). After perfuse fixation, free-floating coronal sections (50 μm) were prepared, and Neurobiotin-labeled neurons were revealed with Cy3-conjugated streptavidin and tested for expression of TH by indirect immunofluorescence (*SI Materials and Methods*). To examine the movement-related firing of dopaminergic neurons, we focused our analyses on brief, self-initiated, spontaneous movements which occurred as a result of the animal adjusting its position on the wheel. Such movements were defined as those involving forelimb movement (determined from video recordings) and with a duration of <1 s. Movement periods were determined using a combination of electromyography (EMG) (measured from cervical muscles) and videos of behavior (30 frames/s). Only neurons recorded during the spontaneous execution of five or more such movement periods were considered for further analysis of movement-related firing. Changes in movement-related activity were considered significant when the firing rate crossed a threshold of the baseline mean ± 2 SD during the defined movement period.

Computational Model of Striatal Dopamine Transmission. We used a computational model of dopamine volume transmission to calculate the extracellular dopamine levels and estimate the activation of postsynaptic signaling cascades (19, 20). The model was driven by spike input of an ensemble of recorded dopaminergic neurons (*SI Materials and Methods*). All movement epochs were averaged to determine the mean single-cell response; then all responses were averaged to obtain mean dopamine concentrations and D1 and D2 receptor activities. In the model, peak dopamine release and uptake scales with the density of release sites; to model the intact mouse dorsolateral striatum, we adjusted innervation to 0.19 terminals/μm^3, which gave a volume-averaged uptake V_{max} = 7.4 μM/s and a dopamine transient evoked by a single pulse of 260 nM (22). To model the ∼30% reduction of evoked dopamine release and ∼30% loss of dopaminergic SNc neurons that develop in aged *SNCA*-OVX mice (28), we reduced the probability of vesicular maximal release from 15 to 10% and the number of neurons driving the model by 30%.

ACKNOWLEDGMENTS. We thank D. Main for performing pilot in vitro voltammetry experiments; A. Kaufmann, J. Kaufling, A. Sharott, and M. Walton for comments on a draft manuscript; and E. Norman, L. Conyers, M. Cioroch, H. Zhang, and J. Janson for expert technical assistance. This work was supported by Medical Research Council UK Awards MC_UU_12020/5 and MC_UU_12024/2 (to P.J.M.) and Award MR/J004324/1 (to S.J.C.), a Monument Trust Discovery Award from Parkinson's UK Grants J-0901 and J-1403, and a Wellcome Trust Investigator Award 101821 (to P.J.M.).

1. Montague PR, Dayan P, Sejnowski TJ (1996) A framework for mesencephalic dopamine systems based on predictive Hebbian learning. *J Neurosci* 16(5):1936–1947.
2. Schultz W, Dayan P, Montague PR (1997) A neural substrate of prediction and reward. *Science* 275(5306):1593–1599.
3. Schultz W (2007) Behavioral dopamine signals. *Trends Neurosci* 30(5):203–210.
4. Matsumoto M, Hikosaka O (2009) Two types of dopamine neuron distinctly convey positive and negative motivational signals. *Nature* 459(7248):837–841.
5. Lammel S, Lim BK, Malenka RC (2014) Reward and aversion in a heterogeneous midbrain dopamine system. *Neuropharmacology* 76(Pt B):351–9.
6. Bromberg-Martin ES, Matsumoto M, Hikosaka O (2010) Dopamine in motivational control: Rewarding, aversive, and alerting. *Neuron* 68(5):815–834.
7. Roeper J (2013) Dissecting the diversity of midbrain dopamine neurons. *Trends Neurosci* 36(6):336–342.
8. Matsumoto M, Takada M (2013) Distinct representations of cognitive and motivational signals in midbrain dopamine neurons. *Neuron* 79(5):1011–1024.
9. Horvitz JC (2000) Mesolimbocortical and nigrostriatal dopamine responses to salient non-reward events. *Neuroscience* 96(4):651–656.
10. Morris G, Nevet A, Arkadir D, Vaadia E, Bergman H (2006) Midbrain dopamine neurons encode decisions for future action. *Nat Neurosci* 9(8):1057–1063.
11. DeLong MR, Crutcher MD, Georgopoulos AP (1983) Relations between movement and single cell discharge in the substantia nigra of the behaving monkey. *J Neurosci* 3(8):1599–1606.
12. Jin X, Costa RM (2010) Start/stop signals emerge in nigrostriatal circuits during sequence learning. *Nature* 466(7305):457–462.
13. Barter JW, Castro S, Sukharnikova T, Rossi MA, Yin HH (2014) The role of the substantia nigra in posture control. *Eur J Neurosci* 39(9):1465–1473.
14. Fan D, Rossi MA, Yin HH (2012) Mechanisms of action selection and timing in substantia nigra neurons. *J Neurosci* 32(16):5534–5548.
15. Schultz W, Ruffieux A, Aebischer P (1983) The activity of pars compacta neurons of the monkey substantia nigra in relation to motor activation. *Exp Brain Res* 51:377–387.
16. Barter JW, et al. (2015) Beyond reward prediction errors: The role of dopamine in movement kinematics. *Front Integr Nuerosci* 9(May):39.
17. Dodson PD, et al. (2015) Distinct developmental origins manifest in the specialized encoding of movement by adult neurons of the external globus pallidus. *Neuron* 86(2):501–513.
18. Björklund A, Dunnett SB (2007) Dopamine neuron systems in the brain: An update. *Trends Neurosci* 30(5):194–202.
19. Dreyer JK, Herrik KF, Berg RW, Hounsgaard JD (2010) Influence of phasic and tonic dopamine release on receptor activation. *J Neurosci* 30(42):14273–14283.
20. Dreyer JK, Hounsgaard J (2013) Mathematical model of dopamine autoreceptors and uptake inhibitors and their influence on tonic and phasic dopamine signaling. *J Neurophysiol* 109(1):171–182.
21. Dreyer JK (2014) Three mechanisms by which striatal denervation causes breakdown of dopamine signaling. *J Neurosci* 34(37):12444–12456.
22. Calipari ES, Huggins KN, Mathews TA, Jones SR (2012) Conserved dorsal-ventral gradient of dopamine release and uptake rate in mice, rats and rhesus macaques. *Neurochem Int* 61(7):986–991.
23. Gerfen CR, Surmeier DJ (2011) Modulation of striatal projection systems by dopamine. *Annu Rev Neurosci* 34:441–466.
24. Beaulieu J-M, Gainetdinov RR (2011) The physiology, signaling, and pharmacology of dopamine receptors. *Pharmacol Rev* 63(1):182–217.
25. Bertran-Gonzalez J, et al. (2008) Opposing patterns of signaling activation in dopamine D1 and D2 receptor-expressing striatal neurons in response to cocaine and haloperidol. *J Neurosci* 28(22):5671–5685.
26. Svenningsson P, et al. (2000) Regulation of the phosphorylation of the dopamine- and cAMP-regulated phosphoprotein of 32 kDa in vivo by dopamine D1, dopamine D2, and adenosine A2A receptors. *Proc Natl Acad Sci USA* 97(4):1856–1860.
27. Marcott PF, Mamaligas AA, Ford CP (2014) Phasic dopamine release drives rapid activation of striatal D2-receptors. *Neuron* 84(1):164–176.
28. Janezic S, et al. (2013) Deficits in dopaminergic transmission precede neuron loss and dysfunction in a new Parkinson model. *Proc Natl Acad Sci USA* 110(42):E4016–E4025.
29. Marinelli M, McCutcheon JE (2014) Heterogeneity of dopamine neuron activity across traits and states. *Neuroscience* 282C:176–197.
30. Lammel S, et al. (2008) Unique properties of mesoprefrontal neurons within a dual mesocorticolimbic dopamine system. *Neuron* 57(5):760–773.
31. Lammel S, Ion DI, Roeper J, Malenka RC (2011) Projection-specific modulation of dopamine neuron synapses by aversive and rewarding stimuli. *Neuron* 70(5):855–862.
32. Beier KT, et al. (2015) Circuit Architecture of VTA Dopamine Neurons Revealed by Systematic Input-Output Mapping. *Cell* 162(3):622–634.
33. Lerner TN, et al. (2015) Intact-Brain Analyses Reveal Distinct Information Carried by SNc Dopamine Subcircuits. *Cell* 162(3):635–647.
34. Brischoux F, Chakraborty S, Brierley DI, Ungless MA (2009) Phasic excitation of dopamine neurons in ventral VTA by noxious stimuli. *Proc Natl Acad Sci USA* 106(12):4894–4899.
35. Cohen JY, Haesler S, Vong L, Lowell BB, Uchida N (2012) Neuron-type-specific signals for reward and punishment in the ventral tegmental area. *Nature* 482(7383):85–88.
36. Ungless MA, Magill PJ, Bolam JP (2004) Uniform inhibition of dopamine neurons in the ventral tegmental area by aversive stimuli. *Science* 303(5666):2040–2042.
37. Brown MTC, Henny P, Bolam JP, Magill PJ (2009) Activity of neurochemically heterogeneous dopaminergic neurons in the substantia nigra during spontaneous and driven changes in brain state. *J Neurosci* 29(9):2915–2925.
38. Joshua M, Adler A, Mitelman R, Vaadia E, Bergman H (2008) Midbrain dopaminergic neurons and striatal cholinergic interneurons encode the difference between reward and aversive events at different epochs of probabilistic classical conditioning trials. *J Neurosci* 28(45):11673–11684.
39. Bayer HM, Glimcher PW (2005) Midbrain dopamine neurons encode a quantitative reward prediction error signal. *Neuron* 47(1):129–141.

40. Lobb CJ, Wilson CJ, Paladini CA (2010) A dynamic role for GABA receptors on the firing pattern of midbrain dopaminergic neurons. *J Neurophysiol* 104(1): 403–413.
41. Henny P, et al. (2012) Structural correlates of heterogeneous in vivo activity of midbrain dopaminergic neurons. *Nat Neurosci* 15(4):613–619.
42. Watabe-Uchida M, Zhu L, Ogawa SK, Vamanrao A, Uchida N (2012) Whole-brain mapping of direct inputs to midbrain dopamine neurons. *Neuron* 74(5):858–873.
43. Sutton RS, Barto AG (1998) *Reinforcement Learning: An Introduction* (MIT Press, Cambridge, MA).
44. Schmitz Y, Schmauss C, Sulzer D (2002) Altered dopamine release and uptake kinetics in mice lacking D2 receptors. *J Neurosci* 22(18):8002–8009.
45. Redgrave P, Prescott TJ, Gurney K (1999) The basal ganglia: A vertebrate solution to the selection problem? *Neuroscience* 89(4):1009–1023.
46. Mink JW (1996) The basal ganglia: Focused selection and inhibition of competing motor programs. *Prog Neurobiol* 50(4):381–425.
47. Kupchik YM, et al. (2015) Coding the direct/indirect pathways by D1 and D2 receptors is not valid for accumbens projections. *Nat Neurosci* 18(9):1230–1232.
48. Tritsch NX, Ding JB, Sabatini BL (2012) Dopaminergic neurons inhibit striatal output through non-canonical release of GABA. *Nature* 490(7419):262–266.
49. Fu Y, et al. (2012) A cytoarchitectonic and chemoarchitectonic analysis of the dopamine cell groups in the substantia nigra, ventral tegmental area, and retrorubral field in the mouse. *Brain Struct Funct* 217(2):591–612.
50. Paxinos G, Franklin KBJ (2013) *The Mouse Brain in Stereotaxic Coordinates* (Elsevier, London), 4th Ed.
51. Holt GR, Softky WR, Koch C, Douglas RJ (1996) Comparison of discharge variability in vitro and in vivo in cat visual cortex neurons. *J Neurophysiol* 75(5):1806–1814.

Supporting Information

Dodson et al. 10.1073/pnas.1515941113

SI Materials and Methods

Experimental Animals. All experimental procedures on animals were conducted in accordance with the Animals (Scientific Procedures) Act, 1986 (United Kingdom). Experiments on wild-type mice were performed using naive 3- to 4-month-old male C57Bl6/J mice ($n = 12$ mice for electrophysiology and $n = 4$ for voltammetry; Charles River Laboratories). Experiments on parkinsonian mice and their controls were carried out blind to genotype using naive 23- to 27-month-old male *SNCA*-OVX mice ($n = 9$) and male $Snca^{-/-}$ littermates ($n = 6$), respectively, all of which were on a C57Bl6/J background. Animals were maintained under a 12/12-h light/dark cycle, and experimental procedures were performed during the light phase of the cycle.

In Vivo Electrophysiological Recording, Juxtacellular Labeling, and Data Analysis. Extracellular recordings were made from individual dopaminergic neurons in head-fixed mice (17). For headpost implantation, mice were anesthetized using 1–2% (vol/vol) isoflurane and were placed in a stereotaxic frame (David Kopf Instruments). The analgesic buprenorphine (Vetergesic; 0.03 mg/kg, s.c.) was administered perioperatively, corneal dehydration was prevented by the application of Hypromellose eye drops (Norton Pharmaceuticals), and the mouse's temperature was maintained using a homeothermic heating mat (Harvard Apparatus). A custom L-shaped stainless steel head-restraint post was affixed to the skull with cyanoacrylate adhesive, positioned so that the 3-mm-diameter hole in its base was above the right substantia nigra (AP −3 mm and ML +1.6 mm in relation to bregma), and a discrete craniotomy was made within the hole. Two 0.8-mm-diameter steel screws were implanted in the skull, one above the left frontal cortex and a reference screw above the left cerebellum. A coiled stainless-steel wire (AM Systems) was implanted between the layers of cervical muscle to record EMG activity (filtered at 0.3–0.5 kHz). The craniotomy was sealed with Kwik-Cast silicone sealant (World Precision Instruments), and the exposed skull and screws were encased in dental acrylic (Jet Denture Repair; Lang Dental).

For electrophysiological recording, mice were placed on top of a custom 22-cm-diameter Ethafoam running wheel, and the head-restraint post was attached to a stereotaxic frame using a custom holder. The recording environment had fixed lighting conditions (~50 lx) and an ambient noise of ~60 decibels. Extracellular recordings of the action potentials (filtered at 0.3–5 kHz; gain of 1,000×; ELX-01MX and DPA-2FS amplifiers from NPI Electronic Instruments) fired by single dopaminergic neurons were made using glass electrodes containing 1.5% (wt/vol) Neurobiotin (Vector Labs) in 0.5 M NaCl (tip diameter ~1.3 μm; 10–30 MΩ in situ). Electrodes were lowered into the brain with submicron precision using a micromanipulator (IVM-1000; Scientifica). Following recording, each neuron was juxtacellularly labeled with Neurobiotin (17, 28). At the end of the experiment, the mouse was deeply anesthetized with pentobarbitone and transcardially perfused with PBS followed by 4% (wt/vol) paraformaldehyde in 0.1 M phosphate buffer. The brain then was removed and placed in 4% paraformaldehyde in 0.1 M phosphate buffer overnight.

To confirm the location and neurochemical identity of recorded and Neurobiotin-labeled neurons, 50-μm coronal sections were cut from the midbrain on a vibrating-blade microtome (VT1000S; Leica Microsystems), collected in series, and washed in PBS. To locate Neurobiotin-labeled cells, free-floating tissue sections were incubated for 4 h at room temperature in PBS with 0.3% (vol/vol) Triton X-100 (Triton PBS; Sigma) containing Cy3-conjugated streptavidin (1:1,000 dilution) (GE Healthcare). Sections containing Neurobiotin-labeled neuronal somata (those marked with Cy3) were tested for the expression of TH immunoreactivity using a rabbit anti-TH antibody (1:1,000) (AB152; Millipore). Sections were washed in PBS and were incubated for 4 h at room temperature in PBS containing fluorophore-conjugated secondary antibodies to visualize immunoreactivity for TH (aminimethylcoumarin-conjugated donkey anti-rabbit IgG; 1:500) (Jackson ImmunoResearch Laboratories). The rabbit anti-TH antibody recognizes a single 60-kDa band corresponding to TH on Western blots of HEK293 cells transfected with cDNA of human TH following the manufacturer's specification; the immunolabeling obtained on sections corresponds to the staining of expected dopaminergic nuclei. Only neurochemically identified dopaminergic neurons (i.e., those expressing TH immunoreactivity) were included in our analyses. The locations of Neurobiotin-labeled neurons were plotted (blind to electrophysiological response) on schematic coronal sections (−2.69 mm to −3.87 mm from bregma, separated by ~100 μm). The SNc was delineated as the compact layer of TH^+ neurons dorsal to the SNr; SNL neurons could be identified as neurons within a cluster of TH^+ neurons lateral to the curvature of the SNr, and VTA dopaminergic neurons could be identified as loosely packed TH^+ neurons dorsal to the medial aspects of the SNc.

All biopotentials were digitized online at 20 kHz with a Power 1401 Analog-Digital converter (Cambridge Electronic Design). Data were acquired and initially analyzed using Spike2 software (version 7.12; Cambridge Electronic Design). Putative single-unit activity was isolated with standard spike-sorting procedures, including template matching, principal component analysis, and supervised clustering (Spike2). Isolation of single units was verified by the presence of a distinct refractory period in the ISI histograms. For analysis of the firing properties of neurons when mice were at rest, periods of movement were removed, and the data were concatenated. The CV2 value (51) was used to assess the regularity of firing (the lower the CV2 value, the more regular was the unit activity).

To examine the movement-related firing of dopaminergic neurons, we focused our analyses on brief, self-initiated, spontaneous movements which occurred as a result of the animal adjusting its position on the wheel. Such movements were defined as those involving forelimb movement (determined from video recordings) and with a duration <1 s. Movement periods were determined using a combination of EMG (measured from cervical muscles) and videos of behavior (30 frames/s), with movement onset marked when the EMG signal exceeded background. Only neurons recorded during the spontaneous execution of such movement periods were considered for further analysis of movement-related firing. For movement-related ISI analysis, mean ISIs occurring during the baseline, premovement (ISIs ending in the 100 ms before movement), and movement (ISIs starting in the 100 ms preceding movement and ending after movement onset) periods were calculated; if fewer than five movements within each period contained ISIs, the cell was excluded from analysis. (For example, if a neuron was recorded during 10 brief movements but failed to spike in the premovement period of seven of these movements, there would be insufficient ISIs for the analysis, and the neuron would be excluded.) In total, we excluded four SNc neurons recorded in wild-type mice and three SNc neurons recorded in *SNCA*-OVX mice from the ISI analysis. Movement duration did not vary by cell-type recorded ($P > 0.05$, ANOVA on ranks) or by genotype ($P > 0.05$, one-way ANOVA). Similarly the number of movement

episodes was not different among cell types ($P > 0.05$, ANOVA on ranks; median = 9 movements for SNc neurons, 8.5 movements for VTA neurons, and 12 movements for SNL neurons; $n = 15$ SNc neurons, 14 VTA neurons, and 5 SNL neurons) or genotypes ($P > 0.05$, ANOVA on ranks; median = 9.5 movements in *Snca*$^{-/-}$ mice and 8.5 movements in *SNCA*-OVX mice; $n = 11$ SNc neurons in *Snca*$^{-/-}$ mice and $n = 12$ neurons in *SNCA*-OVX mice).

PETHs (40-ms bins) were smoothed with a sliding five-point Hamming window using custom MATLAB (MathWorks) routines; varying bin size or smoothing parameters had no systematic effect on the results. To compare movement-related firing across neurons, activity was transformed to z-scores using the baseline mean firing and SD, where baseline was −1,000 to −200 ms relative to movement onset (to avoid possible contamination of baseline with changes in activity just before onset). Premovement periods were considered to be the four bins (160 ms) preceding movement, and movement onset was considered to be the four bins immediately thereafter. Changes in movement-related activity of dopaminergic neurons were considered significant when firing rates crossed a threshold of the baseline mean ± 2 SD during the defined movement period. ROC curves for SNc neurons were constructed as previously described (17) when the firing rate in test epochs (with a duration equal to half the mean movement duration for the analyzed neuron) was less than a series of thresholds. Epochs were moved along the spike train in 10-ms increments, and those straddling the start/end of a movement period were discarded. To assess statistical significance, the AUROC obtained for a given neuron was compared with the 95th percentile of the distribution of AUROCs from 1,000 iterations of shuffled data generated by shifting movement periods to random positions within the recording.

Computational Model of Striatal Dopamine Transmission. We used a computational model of dopamine volume transmission to calculate the extracellular dopamine levels and estimate the activation of postsynaptic signaling cascades (19, 20). The model incorporates probabilistic vesicular release, diffusion in extracellular space, and reuptake by dopaminergic axons and was driven by spike input of an ensemble of recorded dopaminergic neurons.

For each recorded dopaminergic neuron, we selected spikes in a 5-s time interval around each move (4 s before and 1 s after); spikes first were binned in 10-ms bins and then were smoothed by a Gaussian kernel (70 ms SD). The resulting continuous firing rate was used as input for independent inhomogeneous Poisson processes driving the spikes of the ensemble. All movement epochs were averaged to determine the mean single-cell response for dopamine release and D1 and D2 receptor activation. Final average dopamine concentrations and receptor activities were obtained from the average of all mean single-cell responses and were generated from each set of neuronal ensembles (e.g., the mean of the individual responses generated from the 15 SNc neurons in wild-type mice). The SD was calculated as the square root of the pooled variance, i.e., as the sum of variance for each cell weighted by the number of movements for the cell.

In the model, peak dopamine release and uptake scale with the density of dopamine release sites. When modeling the intact dorsolateral striatum, we adjusted the dopaminergic innervation to 0.19 terminals/μm^3, giving a volume-averaged uptake V_{max} = 7.4 μM/s and a dopamine transient evoked by a single pulse of 260 nM (22). Uptake per terminal, autoreceptors, and minimum and maximum vesicular release probabilities for each terminal were as in previous applications of the model (19, 20).

Overexpression of human α-synuclein in *SNCA*-OVX mice leads to an ∼30% reduction of evoked dopamine release and to an additional ∼30% loss of TH$^+$ SNc neurons in aged mice (28). We modeled these changes, respectively, by a reduction of vesicular maximal release probability from 15% to 10%, and by a 30% reduction in the number of neurons driving the model (leading to a 30% reduction in innervation). Dopamine signaling in the nucleus accumbens was simulated using previously used innervation density and uptake parameters.

FCV Measurement of Dopamine Release in the Dorsal Striatum. Acute brain slices (coronal, 300 μm) containing dorsal striatum were prepared in ice-cold Hepes Ringer's solution (in mM: 120 NaCl, 5 KCl, 20 NaHCO3, 6.7 Hepes acid, 3.3 Hepes salt, 2 CaCl2, 2 $MgSO_4$, 1.2 KH_2PO_4 and 10 glucose saturated with 95% O2/5% CO_2) using a vibrating-blade microtome (VT1000S; Leica Microsystems). For recordings, slices were transferred to bicarbonate-buffered artificial CSF at ∼1.5 mL/min and 30–32 °C (in mM: 124 NaCl, 3.7 KCl, 26 NaHCO3, 2.4 CaCl2, 1.3 $MgSO_4$, 1.3 KH_2PO_4, and 10 glucose saturated with 95% O2/5% CO_2). The nicotinic receptor antagonist DHβE (1 μM) was included throughout to prevent the effects of direct stimulation of striatal cholinergic interneurons on dopamine transmission. Voltammetric recordings were made using a Millar Voltammeter (Julian Millar, Barts and the London School of Medicine and Dentistry, London) and were acquired and analyzed using AxoScope (Molecular Devices). Voltammograms were obtained by scanning with a triangular waveform (–0.7 to +1.3 V to –0.7 V versus Ag/AgCl switching to 0 V between scans; 800 V/s; 8 Hz). Evoked extracellular concentrations of dopamine were measured using FCV with carbon fiber microelectrodes (CFMs) constructed in-house (fiber tip diameter, ∼7 μm; exposed fiber length, 50–100 μm) and positioned ∼100 μm into the tissue. Electrode calibrations were performed after recordings for each electrode using 2 μM dopamine. A concentric bipolar stimulating electrode (FHC, Inc.) was positioned on the tissue surface 50–100 μm from the CFM to evoke striatal dopamine release electrically. Monophasic stimulus pulses (0.2-ms duration; 0.67 mA) were delivered out-of-phase with FCV scans. Stimulus trains were repeated at intervals of 5 min and consisted of ∼11 s of stimulation at an average frequency of 6 Hz. Once a steady-state dopamine level had been reached (after ∼7 s), a pause of 277 ms was introduced into the stimulus train. This pause duration was chosen to approximate the pause in the firing of SNc dopaminergic neurons recorded in vivo and to avoid clashes between subsequent stimulation pulses and voltage scans. Dopamine oxidation currents were measured from background-subtracted voltammograms and converted to concentration using the calibration factor for the CFM used. At least three replicate recordings were made per striatal recording site and were averaged to produce an observation for that site (data from each site were treated independently for statistical analysis). Baseline values of dopamine release were calculated from the mean dopamine concentration of the 0.5 s immediately preceding pause onset and were compared with the 0.5 s following pause onset. For plotting, data were normalized to baseline and smoothed with a sliding five-point Hamming window.

Statistical Analyses. Before statistical comparison, data were tested for equal variance and normality (Shapiro–Wilk test, $P < 0.05$ to reject). For normally distributed, homoscedastic datasets, comparisons were made using two-tailed Student's t tests; for all other data, Mann–Whitney rank sum tests were used (SigmaStat; Systat Software Inc.). Multiple comparisons of normally distributed data were performed using one-way ANOVA or one-way repeated measures ANOVA with Dunnett's post hoc comparison with control. For multiple comparisons of nonnormally distributed data, a Kruskal–Wallis one-way ANOVA on ranks with Dunn's post hoc test was used. Data are presented as mean ± SEM throughout.

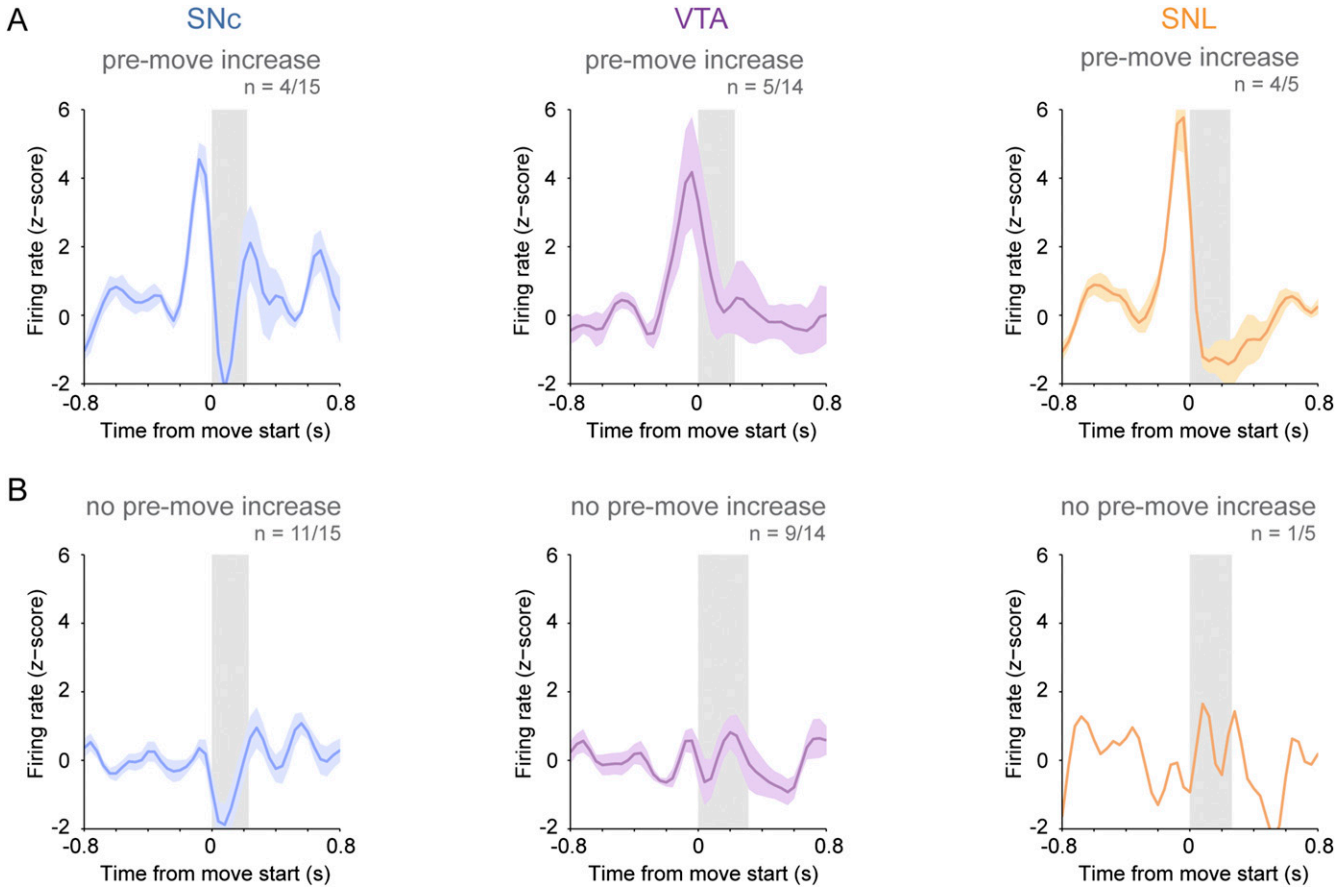

Fig. S1. A minority of dopaminergic neurons in the SNc and VTA and the majority of dopaminergic neurons in the SNL increase firing just before movement onset. Shown are mean normalized PETHs ± SEM of neurons exhibiting significant increases in firing rate (*A*) or no change in in firing rate (*B*) just before movement onset.

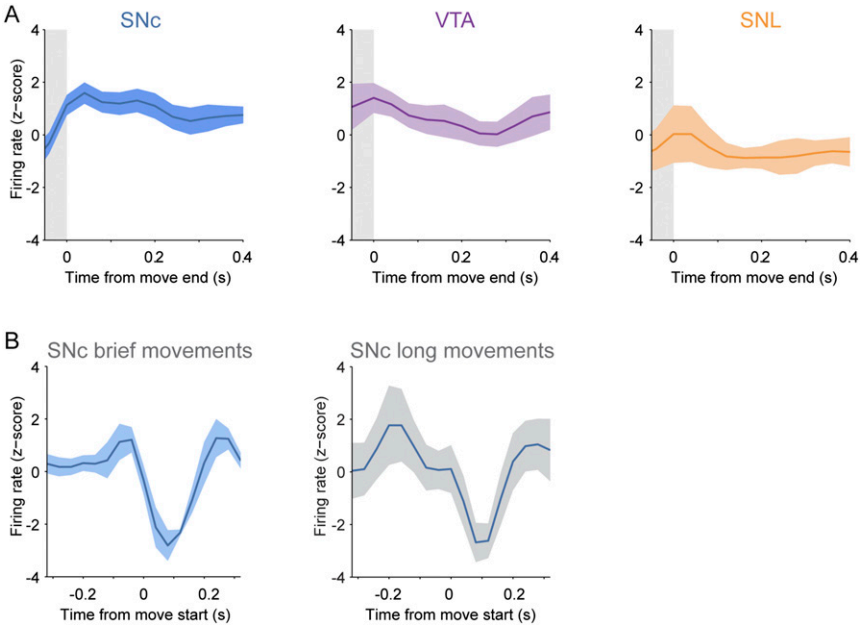

Fig. S2. Dopaminergic neurons do not reliably represent the termination of brief movements, but SNc neurons represent the onset of longer movements. (*A*) Mean normalized PETHs ± SEM aligned to the end of each movement period (gray shading) for SNc, VTA, or SNL neurons show that, on average, these types of dopaminergic neurons do not alter their firing rates significantly at the end of movement (n = 15 SNc neurons, 14 VTA neurons, and 5 SNL neurons). (*B*) Mean normalized PETHs ± SEM aligned to the start of each movement for a set of SNc neurons (n = 5) that were recorded during both brief (*Left*) and longer (*Right*) movements. Note that the decreased firing of these neurons that occurred at the onset of brief movements also occurred at the onset of the long movements. Data for long-duration movements were pooled across neurons (13 movements, mean duration 35.87 ± 6.55 s).

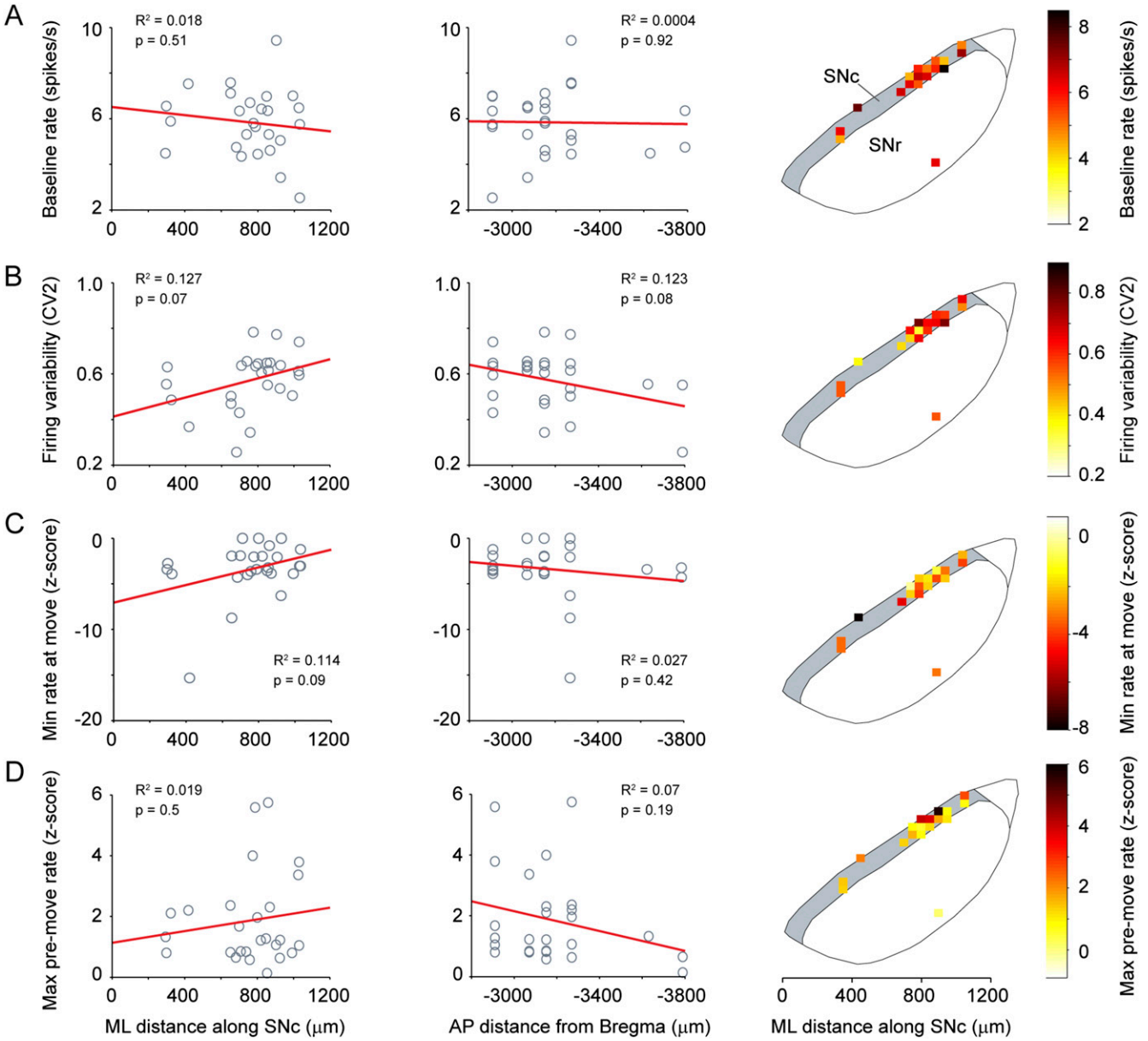

Fig. S3. Firing properties of SNc neurons are not related to their location within the nucleus. (*A–D*, *Left* and *Center*) Firing properties [baseline firing rate (*A*), variability in firing rate (*B*), minimum firing rate at movement (*C*), and maximum firing rate premovement (*D*)] of SNc neurons from wild-type and *Snca*$^{-/-}$ mice were plotted according to their ML (*Left*) or AP (*Center*) positions in the SNc and were fit with a least-squares regression. R^2 and *P* values from a Pearson product–moment correlation ($n = 26$ SNc neurons) are given. (*A–D*, *Right*) Firing property heat maps were constructed by dividing the SNc into 50-μm^2 segments. The color represents the mean value of all neurons within each segment. There were no significant relationships between ML or AP position or the mean firing rate of SNc dopamine neurons during the baseline period before movement (*A*), firing variability at rest (*B*), the minimum z-scored firing rate reached in the 160 ms following the start of movement onset (*C*), or the maximum z-scored firing rate during the 160 ms preceding movement (*D*).

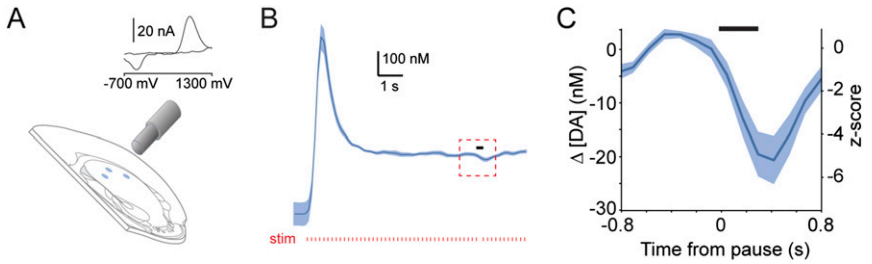

Fig. S4. Brief pauses significantly alter the extracellular dopamine concentration in dorsal striatum ex vivo. (*A*) Schematic of dopamine measurement in the dorsal striatum by FCV as used to determine the change in dopamine concentration associated with a brief pause in stimulation. (*Inset*) An example of a voltammogram. (*B*) Mean extracellular dopamine concentration (blue; SEM indicated by shading) elicited by a train of electrical stimuli (red ticks) delivered to dorsal striatum at 6 Hz (the approximate rate of firing of SNc neurons when animals were at rest). A brief pause in stimulation (denoted by black bar; 277-ms duration, mimicking the ISI of SNc neurons at movement onset) was introduced ~7 s after the start of stimulation when the dopamine levels had reached a steady state. (*C*) Mean change in extracellular dopamine concentration in response to the 277-ms pause (black bar; see red box in *B*). The dopamine concentration was significantly lower in the 0.5 s following the initiation of the pause than during 0.5 s of baseline stimulation ($P = 0.001$, paired t test; $n = 10$ recording sites).

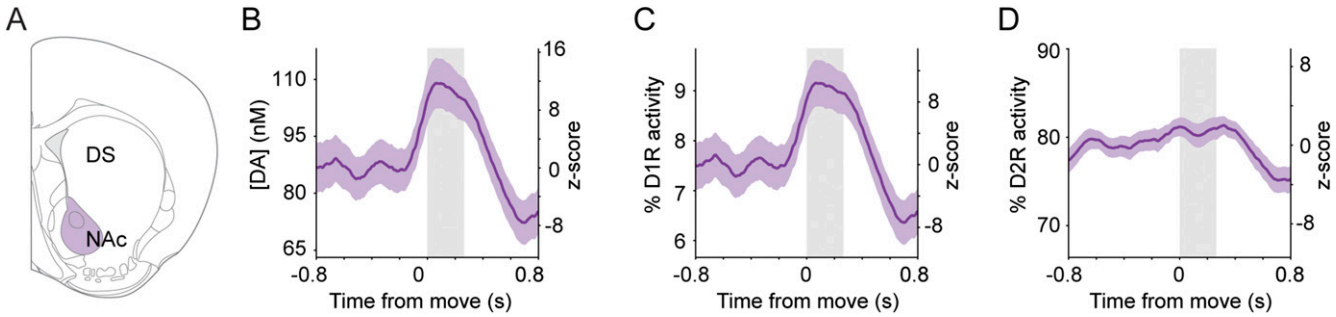

Fig. S5. Computational modeling predicts that the movement-related firing of VTA dopaminergic neurons will lead to a peak in dopamine release in the nucleus accumbens during movement. (*A*) Schematic illustrating the region in which dopamine release and receptor activity were modeled using spike trains recorded from VTA neurons. DS, dorsal striatum; NAc, nucleus accumbens. (*B–D*) Movement-related changes (mean PETH ± SEM) in dopamine concentration (*B*), in the activity of low-affinity D1 dopamine receptors (*C*), and in the activity of high-affinity D2 dopamine receptors (*D*) in the nucleus accumbens.

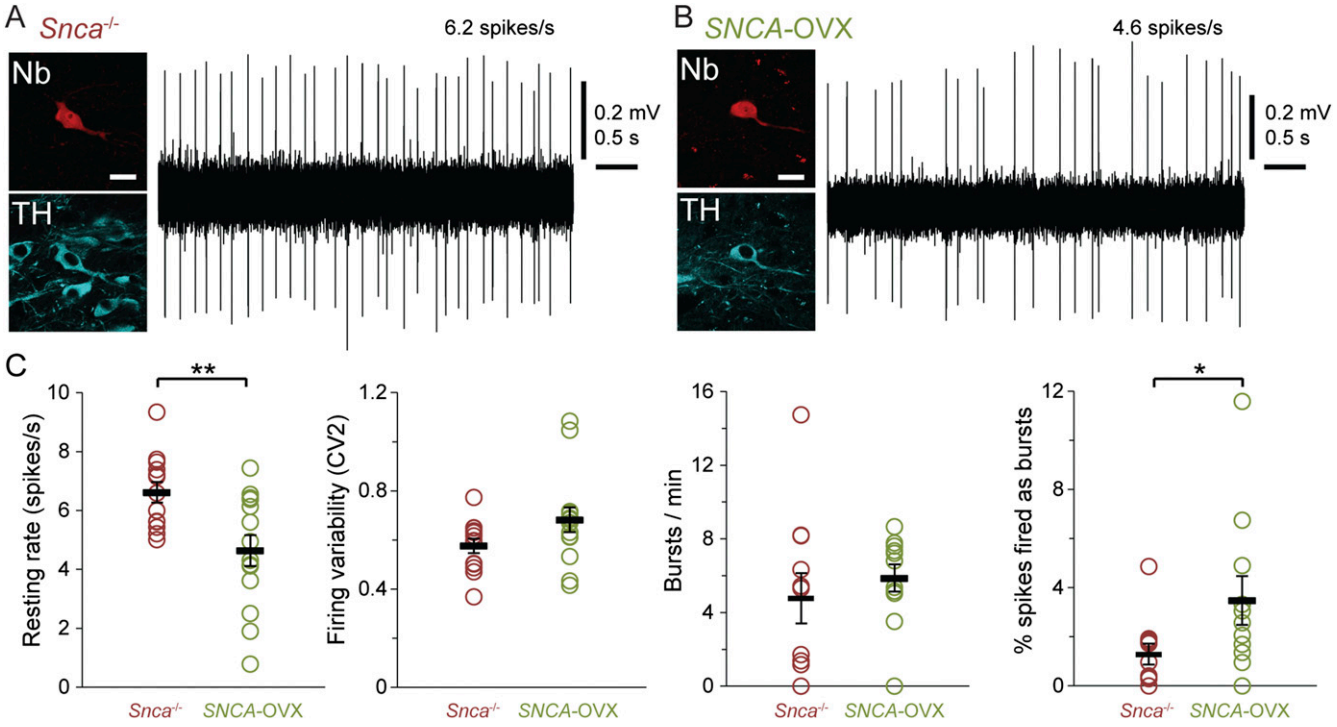

Fig. S6. Dopaminergic SNc neurons have abnormally low firing rates in aged parkinsonian mice at rest. (*A* and *B*) Typical single-unit activities recorded from identified dopaminergic SNc neurons in 24-month-old *Snca*$^{-/-}$ littermate controls (*A*) or *SNCA*-OVX parkinsonian mice (*B*) during alert rest. After recording, individual neurons were juxtacellularly labeled with Neurobiotin (Nb); dopaminergic identity was verified by the expression of TH. (Scale bars, 20 μm.) (*C*) In vivo firing properties of SNc neurons in *Snca*$^{-/-}$ and *SNCA*-OVX mice during alert rest. The mean firing rate was significantly lower in *SNCA*-OVX mice ($P < 0.01$, *t* test), but firing variability was similar across the genotypes ($P > 0.05$, Mann–Whitney test). The number of bursts per minute fired by neurons was not significantly different across genotypes ($P > 0.05$, *t* test), but SNc neurons in *SNCA*-OVX mice fired a higher percentage of spikes as bursts ($P < 0.05$, Mann–Whitney test). Data are presented as mean ± SEM plotted (thick black bar and error bars); $n = 13$ neurons from *Snca*$^{-/-}$ mice and 14 neurons from *SNCA*-OVX mice. *$P < 0.05$, **$P < 0.01$.